

FIG. S1. A comparison of pddfs, and respectively of SAS intensities for different α -shapes, where $r_{\max} = 6 \text{ \AA}$. Black - analytical results, red - simulation data using α -SAS method. (a) Pddf from a cube of edge length $L = 40 \text{ \AA}$. (b) SAS of the same cube with form factor given in Table S1. (c) Pddf from a sphere of radius $a = 20 \text{ \AA}$. (d) SAS of the same sphere with the form factor given in Table S1. (e) Monte Carlo simulations of 100 pddfs for an α -cylinder. The radius and height of the embedding cylinder are $a = 20 \text{ \AA}$, and $L_0 = 80 \text{ \AA}$. The averages of pddfs are reported in Fig. 1e - green line. (f) The corresponding SAS intensities. Their average is reported in Fig. 1f - green line.

TABLE S1. Analytical expressions of radius of gyration for common shapes.

Shape	Radius of gyration	Form factor
Cylinder of radius a and height L (Svergun et al., 2013)	$R_g^{\text{th}} = \left(\frac{a^2}{2} + \frac{L^2}{12} \right)^{1/2}$	$\frac{\sin(qL2^{-1}\sin\psi)}{qL2^{-1}\sin\psi} \frac{2J_1(qa\cos\psi)}{qa\cos\psi}, q = \mathbf{q} ^a$
Cube of edge length L (Svergun et al., 2013)	$R_g^{\text{th}} = L/2$	$\frac{\sin(q_x L/2)}{q_x L/2} \frac{\sin(q_y L/2)}{q_y L/2} \frac{\sin(q_z L/2)}{q_z L/2} b$
Sphere of radius a (Svergun et al., 2013)	$R_g^{\text{th}} = a \left(\frac{3}{5} \right)^{1/2}$	$3 \frac{\sin(qa) - qa\cos(qa)}{(qa)^3}, q = \mathbf{q} $
Janus particles ^c of radius a (Kaya, 2002)	$R_g^{\text{th}} = \left(\frac{3}{5}a^2 - \frac{9}{64} \left(\frac{\Delta\rho_1 - \Delta\rho_2}{\Delta\rho_1 + \Delta\rho_2} \right)^2 a^2 \right)^{1/2}$	Eq. (7)

^a $J_1(\cdot)$ is the first order Bessel function of the first kind

^b q_x, q_y and q_z are the components of the momentum transfer \mathbf{q}

^c with contrasts $\Delta\rho_1$ and $\Delta\rho_2$ for the two hemispheres

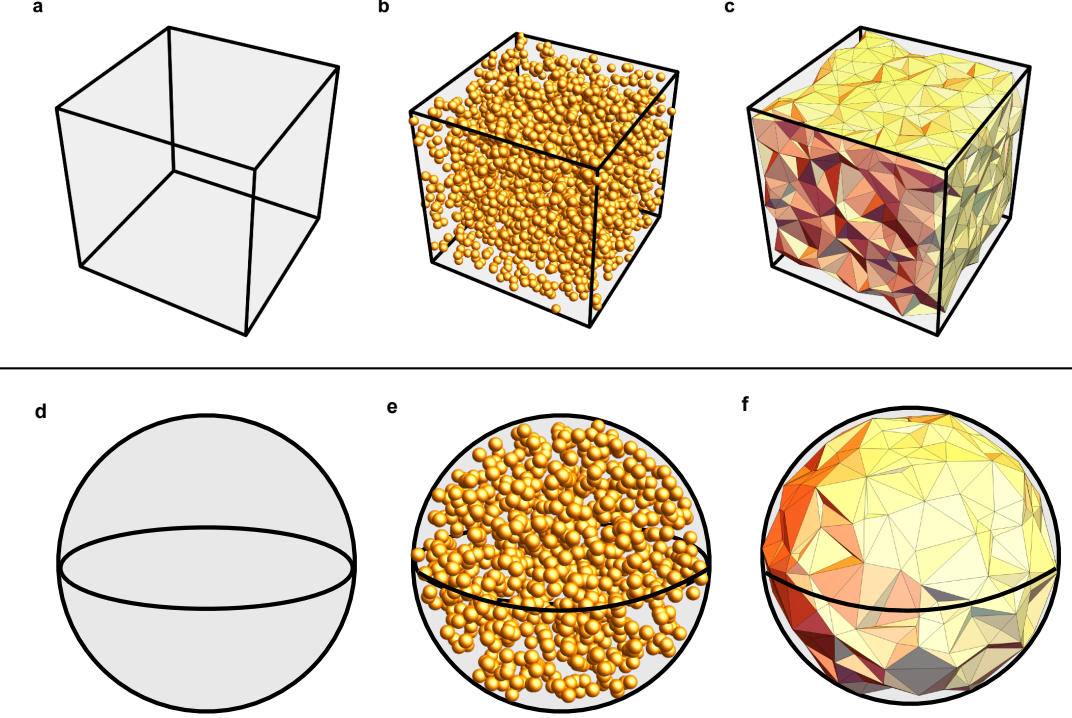


FIG. S2. Construction process of α -shapes for different structures. (a-c) Cubes, and (d-f) spheres. First, the sampling volume is set (a and d). Second, a collection of randomly distributed points is generated within the respective volumes (b and e). Third, the α -shape is generated as an "envelope" of these points. Note that in both cases, from its definition (Section 2.1) it follows that the α -shape is slightly smaller (on average about 4 % at the value of $r_{\max} \equiv 1/\alpha = 6 \text{ \AA}$ used here; see main text for details) as compared to the envelope.

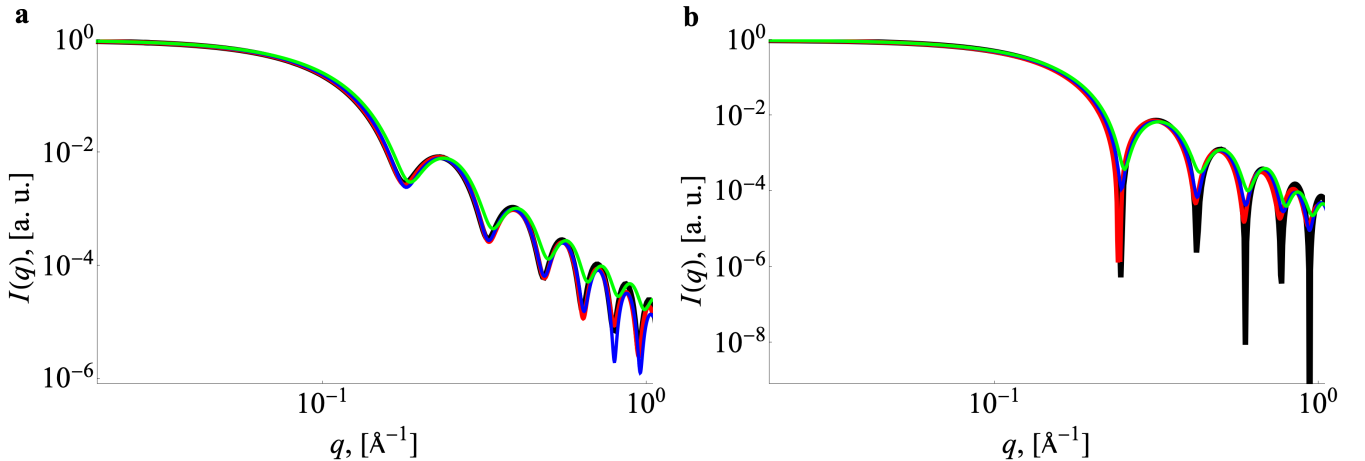


FIG. S3. A comparison of scattering intensities for different number of points used in building the α -shape. (a) Cubes. (b) Spheres. The parameters are the same as in Fig. 1. Black - analytical curve. Green, blue and red - simulated curves using α -SAS method with 3×10^4 , 3.5×10^4 and respectively 4×10^4 points.

TABLE S2. Structural parameters of Janus particles with radius $R = 50 \text{ \AA}$. The SLD of the background/solvent/solution is fixed at $\rho_0 = 0 \text{ (} 10^{10} \text{ cm}^{-2} \text{)}$ and the SLD of one region, red coloured hemisphere in Fig. 3a-f, is fixed at $\rho_2 = 1 \text{ (} 10^{10} \text{ cm}^{-2} \text{)}$. The scattering intensity is normalized to 1 at $q = 0$.

$\eta^{\text{a}} (\%)$	$\rho_1^{\text{b}} (10^{10} \text{ cm}^{-2})$	$R_g^{\text{thc}} (\text{\AA})$	$R_g^{\text{d}} (\text{\AA})$	$R_{g1}^{\text{e}} (\text{\AA})$	$R_{g2}^{\text{f}} (\text{\AA})$	$I_1(0)^{\text{g}}$	$I_2(0)^{\text{h}}$	$I_{12}(0)^{\text{i}}$
0	0	33.89	33.84 ± 0.02	0	33.84 ± 0.02	0	100	0
10	10	35.56	34.46 ± 0.03	30.93 ± 0.03	33.73 ± 0.03	0.09	94.00	5.91
20	20	36.66	36.08 ± 0.04	32.44 ± 0.04	33.71 ± 0.04	1.86	74.60	23.54
30	30	37.39	37.10 ± 0.03	32.94 ± 0.03	33.71 ± 0.03	4.08	63.69	32.23
40	40	37.89	37.71 ± 0.03	33.09 ± 0.03	33.68 ± 0.03	6.88	54.41	38.71
50	50	38.22	38.16 ± 0.04	33.16 ± 0.04	33.71 ± 0.04	10.54	45.61	43.85
60	60	38.45	38.45 ± 0.04	33.41 ± 0.04	33.67 ± 0.04	12.47	41.83	45.70
70	70	38.59	38.58 ± 0.03	33.40 ± 0.03	33.62 ± 0.03	16.53	35.21	48.26
80	80	38.67	38.74 ± 0.03	33.43 ± 0.03	33.67 ± 0.03	19.40	31.31	49.29
90	90	38.72	38.78 ± 0.03	33.55 ± 0.03	33.65 ± 0.03	22.17	27.30	50.53
100	100	38.73	38.85 ± 0.02	33.59 ± 0.02	33.65 ± 0.02	24.96	25.03	50.01

^a contrast parameter defined by Eq. (6)

^b SLD of region 2 (blue hemisphere in Fig. 3a-f), calculated with Eq. (6)

^c theoretical radius of gyration calculated with the expression from Tab. I (4-th row)

^d radius of gyration calculated with Eq. (3) for the whole Janus particle

^e radius of gyration calculated with Eq. (3) for region 1 (blue hemisphere in Fig. 3a-f)

^f radius of gyration calculated with Eq. (3) for region 2 (red hemisphere in Fig. 3a-f)

^g forward intensity of region 1 (blue hemisphere in Fig. 3a-f)), from Eq. (4), (units: % $\times I(0)$)

^h forward intensity of region 2 (red hemisphere in Fig. 3a-f)), from Eq. (4), (units: % $\times I(0)$)

ⁱ correlations between region 1 and region 2 of JP (Fig. 3a-f), from Eq. (4), (units: % $\times I(0)$)

TABLE S3. Structural parameters of KinA-2Sda complex.

$f_{\text{D}_2\text{O}}^{\text{a}} (\%)$	$c^{\text{b}} (\text{mg/mL})$	$\rho^{\text{c}} (10^{10} \text{ cm}^{-2})$	$\Delta\rho^{\text{d}} (10^{10} \text{ cm}^{-2})$	$R_g^{\text{e}} (\text{\AA})$	$D_{\max}^{\text{f}} (\text{\AA})$	$I(0)^{\text{g}} (\text{cm}^{-1})$
0	11.9	-0.511	2.980	28.07 ± 0.04	77.75 ± 0.11	0.617
10	11.9	0.174	2.420	28.26 ± 0.04	77.34 ± 0.11	0.409
20	11.9	0.858	1.860	28.50 ± 0.03	76.94 ± 0.11	0.244
30	-	1.543	1.300	28.46 ± 0.03	75.76 ± 0.11	-
40	26.6	2.227	0.740	22.15 ± 0.04	69.33 ± 0.13	0.090
50	-	2.912	0.180	28.51 ± 0.06	75.93 ± 0.16	-
60	-	3.596	-0.380	27.96 ± 0.07	77.52 ± 0.19	-
70	-	4.281	-0.940	27.34 ± 0.07	78.23 ± 0.20	-
80	11.9	4.965	-1.500	23.94 ± 0.08	77.97 ± 0.26	0.149
90	11.9	5.650	-2.060	24.17 ± 0.06	78.64 ± 0.20	0.285
100	11.9	6.334	-2.620	25.66 ± 0.04	78.73 ± 0.12	0.464

^a deuterium content of the solvent

^b concentration of KinA+2Sda

^c SLD of the solvent (200 mM NaCl + 50 mM Tris + 150 mM imidazole), calculated with Eq. (14)

^d total contrast, given by Eq. (15)

^e radius of gyration calculated with Eq. (3) for the whole KinA+2Sda complex

^f maximum diameter (D_{\max}) obtained from the condition that $p(r) \rightarrow 0$ when $r = D_{\max}$ in Eq. (3)

^g forward intensity of KinA+2Sda complex, given by Eq. (10)

TABLE S4. Structural parameters of KinA subunit.

f_{D_2O} ^a (%)	ρ^b (10^{10} cm^{-2})	$\Delta\rho^c$ (10^{10} cm^{-2})	R_g^d (\AA)	D_{\max}^e (\AA)	$I(0)^f$ (% $\times I(0)$)
0	1.759	2.270	25.92 ± 0.03	79.11 ± 0.09	63.73
10	1.879	1.706	25.93 ± 0.03	79.11 ± 0.09	58.44
20	1.999	1.141	25.93 ± 0.03	78.94 ± 0.09	50.22
30	2.120	0.577	25.92 ± 0.03	78.83 ± 0.09	32.72
40	2.240	0.013	25.71 ± 0.04	81.82 ± 0.13	0.131
50	2.360	-0.552	25.91 ± 0.04	78.94 ± 0.12	39.53
60	2.480	-1.116	26.02 ± 0.03	79.13 ± 0.09	64.42
70	2.600	-1.680	25.98 ± 0.03	79.15 ± 0.09	77.71
80	2.721	-2.245	25.99 ± 0.03	79.14 ± 0.09	86.09
90	2.841	-2.809	26.01 ± 0.03	79.16 ± 0.09	91.66
100	2.961	-3.373	26.00 ± 0.03	79.15 ± 0.09	95.46

^a deuterium content of the solvent^b SLD calculated with Eq (14)^c contrast, calculated with Eq (15)^d radius of gyration calculated with Eq. (3)^e maximum diameter (D_{\max}) obtained from the condition that $p(r) \rightarrow 0$ when $r = D_{\max}$ in Eq. (3)^f^f forward intensity expressed as percents from the total intensity given in Table S3 last column

TABLE S5. Structural parameters of 2Sda subunit.

f_{D_2O} ^a (%)	ρ^b (10^{10} cm^{-2})	$\Delta\rho^c$ (10^{10} cm^{-2})	R_g^d (\AA)	D_{\max}^e (\AA)	$I(0)^f$ (% $\times I(0)$)
0	5.716	6.227	21.10 ± 0.03	62.32 ± 0.09	4.072
10	5.860	5.686	21.10 ± 0.03	62.45 ± 0.09	5.551
20	6.004	5.146	21.10 ± 0.03	62.42 ± 0.09	8.484
30	6.149	4.606	21.09 ± 0.03	62.56 ± 0.09	18.32
40	6.293	4.660	21.10 ± 0.04	62.51 ± 0.12	92.89
50	6.437	3.525	21.10 ± 0.04	62.57 ± 0.12	13.78
60	6.581	2.985	21.11 ± 0.04	62.48 ± 0.12	3.894
70	6.726	2.445	21.10 ± 0.03	62.26 ± 0.09	1.402
80	6.870	1.905	21.10 ± 0.03	62.47 ± 0.09	0.526
90	7.014	1.364	21.09 ± 0.03	62.53 ± 0.09	0.184
100	7.129	0.824	21.11 ± 0.03	63.22 ± 0.09	0.054

^a deuterium content of the solvent^b SLD calculated with Eq (14)^c contrast, calculated with Eq (15)^d radius of gyration calculated with Eq. (3)^e maximum diameter (D_{\max}) obtained from the condition that $p(r) \rightarrow 0$ when $r = D_{\max}$ in Eq. (3)^f^f forward intensity expressed as percents from the total intensity given in Table S3 last column

TABLE S6. Structural parameters of R1-3 human dystrophin - nanodisk complex, at concentration $c = 4.2 \text{ mg/mL}$.

$f_{\text{D}_2\text{O}}^{\text{a}} (\%)$	$\rho^{\text{b}} (10^{10} \text{ cm}^{-2})$	$\Delta\rho^{\text{c}} (10^{10} \text{ cm}^{-2})$	$R_g^{\text{d}} (\text{\AA})$	$D_{\max}^{\text{e}} (\text{\AA})$	$I(0)^{\text{f}} (\text{cm}^{-1})$
0	-0.544	2.385	41.24 ± 0.09	141.97 ± 0.93	0.912
10	0.148	1.827	41.73 ± 0.09	141.73 ± 0.48	0.545
20	0.839	1.270	42.32 ± 0.08	141.97 ± 0.91	0.263
30	1.531	0.712	42.86 ± 0.08	141.71 ± 0.65	0.086
40	2.223	0.154	38.87 ± 0.10	141.97 ± 1.82	0.011
50	2.915	-0.403	42.06 ± 0.08	141.78 ± 2.97	0.032
60	3.606	-0.961	42.86 ± 0.09	141.73 ± 2.12	0.153
70	4.298	-1.519	42.56 ± 0.09	141.25 ± 0.59	0.372
80	4.990	-2.076	42.33 ± 0.08	141.56 ± 0.72	0.701
90	5.081	-2.634	35.08 ± 0.09	141.82 ± 0.66	1.135
100	6.373	-3.191	41.93 ± 0.09	141.73 ± 0.81	1.664

^a deuterium content of the solvent^b SLD of the solvent (150 mM NaCl + 20 mM Tri-d11 + 0.1 mM EDTA-d16), calculated with Eq. (17)^c total contrast, given by Eq. (18)^d radius of gyration calculated with Eq. (3) for the whole R1-3 human dystrophin - nanodisk complex^e maximum diameter (D_{\max}) obtained from the condition that $p(r) \rightarrow 0$ when $r = D_{\max}$ in Eq. (3)^f forward intensity of R1-3 human dystrophin - nanodisk complex, given by Eq. (10)TABLE S7. Structural parameters of R1-3 human dystrophin, at concentration $c = 4.2 \text{ mg/mL}$.

$f_{\text{D}_2\text{O}}^{\text{a}} (\%)$	$\rho^{\text{b}} (10^{10} \text{ cm}^{-2})$	$\Delta\rho^{\text{c}} (10^{10} \text{ cm}^{-2})$	$R_g^{\text{d}} (\text{\AA})$	$D_{\max}^{\text{e}} (\text{\AA})$	$I(0)^{\text{f}} (\text{cm}^{-1})$
0	1.843	2.387	39.78 ± 0.08	141.97 ± 0.93	0.757
10	1.978	1.830	39.77 ± 0.09	141.73 ± 0.48	0.414
20	2.112	1.273	39.76 ± 0.08	141.97 ± 0.91	0.174
30	2.247	0.715	39.77 ± 0.09	141.71 ± 0.65	0.041
40	2.381	0.158	39.87 ± 0.09	141.97 ± 1.82	0.011
50	2.515	-0.399	39.72 ± 0.07	141.78 ± 2.97	0.001
60	2.650	-0.956	39.77 ± 0.09	141.73 ± 2.12	0.039
70	2.784	-1.514	39.76 ± 0.08	141.25 ± 0.59	0.223
80	2.919	-2.071	39.77 ± 0.08	141.56 ± 0.72	0.463
90	3.053	-2.628	39.81 ± 0.08	141.82 ± 0.66	0.034
100	3.188	-3.186	39.76 ± 0.09	141.73 ± 0.81	1.198

^a deuterium content of the solvent^b SLD calculated with Eq. (17)^c total contrast, given by Eq. (18)^d radius of gyration calculated with Eq. (3) for the R1-3 hyman dystrophin^e maximum diameter (D_{\max}) obtained from the condition that $p(r) \rightarrow 0$ when $r = D_{\max}$ in Eq. (3)^f forward intensity expressed as percents from the total intensity given in Table S6 last columnTABLE S8. Structural parameters of the nanodisk, with SLD $\rho = 0.720 \times 10^{10} \text{ cm}^{-2}$.

$f_{\text{D}_2\text{O}}^{\text{a}} (\%)$	$\Delta\rho^{\text{b}} (10^{10} \text{ cm}^{-2})$	$R_g^{\text{c}} (\text{\AA})$	$D_{\max}^{\text{d}} (\text{\AA})$	$I(0)^{\text{e}} (\text{cm}^{-1})$
0	1.264	27.12 ± 0.07	79.24 ± 0.76	0.007
10	0.573	27.13 ± 0.07	79.31 ± 0.44	0.009
20	-0.119	27.15 ± 0.08	79.01 ± 0.64	0.009
30	-0.811	27.18 ± 0.07	79.09 ± 0.83	0.008
40	-1.503	27.24 ± 0.08	79.41 ± 0.27	0.001
50	-2.194	27.21 ± 0.08	79.56 ± 1.43	0.007
60	-2.886	27.19 ± 0.09	79.04 ± 0.88	0.014
70	-3.578	27.19 ± 0.07	79.09 ± 0.54	0.019
80	-4.270	27.14 ± 0.08	79.01 ± 0.43	0.028
90	-4.961	27.27 ± 0.09	79.41 ± 0.54	0.768
100	-5.653	27.11 ± 0.08	78.98 ± 0.86	1.212

^a deuterium content of the solvent^b total contrast, given by Eq. (18)^c radius of gyration calculated with Eq. (3) for the whole nanodisk^d maximum diameter (D_{\max}) obtained from the condition that $p(r) \rightarrow 0$ when $r = D_{\max}$ in Eq. (3)^e forward intensity expressed as percents from the total intensity given in Table S6 last column

TABLE S9. Structural parameters of RBD-Sb23 complex.

$f_{D_2O}^a$ (%)	c^b (mg/mL)	ρ^c (10^{10} cm $^{-2}$)	$\Delta\rho^d$ (10^{10} cm $^{-2}$)	R_g^e (Å)	D_{max}^f (Å)	$I(0)^g$ (cm $^{-1}$)
0	11.9	-0.548	3.791	28.70 ± 0.07	120.04 ± 0.29	0.703
10	11.9	0.144	3.233	27.91 ± 0.07	120.11 ± 0.30	0.514
20	11.9	0.836	2.675	26.65 ± 0.07	119.34 ± 0.31	0.354
30	11.9	1.528	2.117	24.38 ± 0.09	118.33 ± 0.44	0.223
40	26.6	2.220	1.559	19.28 ± 0.09	111.42 ± 0.52	0.274
50	11.9	2.912	1.001	14.04 ± 0.10	55.58 ± 3.97	0.052
60	11.9	3.604	0.443	27.27 ± 0.07	119.83 ± 3.08	0.011
70	52.3	4.296	-0.115	30.40 ± 0.07	121.25 ± 0.28	0.001
80	11.9	4.988	-0.673	31.67 ± 0.07	120.81 ± 0.27	0.020
90	11.9	5.680	-1.232	31.53 ± 0.07	119.67 ± 0.27	0.070
100	11.9	6.372	-1.790	30.25 ± 0.08	116.73 ± 0.31	0.150

^a deuterium content of the solvent^b concentration of RBD+Sb23 (the values were taken similar to those for KinA+2Sda in Table S3 second column, including for the missing ones)^c SLD of the solvent (100 mM NaCl + 25 mM Tris), calculated with Eq. (20)^d total contrast, given by Eq. (21)^e radius of gyration calculated with Eq. (3) for the whole RBD+Sb23 complex^f maximum diameter (D_{max}) obtained from the condition that $p(r) \rightarrow 0$ when $r = D_{max}$ in Eq. (3)^g forward intensity of RBD-Sb23 complex, given by Eq. (10)

TABLE S10. Structural parameters of RBD subunit.

$f_{D_2O}^a$ (%)	ρ^b (10^{10} cm $^{-2}$)	$\Delta\rho^c$ (10^{10} cm $^{-2}$)	R_g^d (Å)	D_{max}^e (Å)	$I(0)^f$ (cm $^{-1}$)
0	1.947	2.495	27.32 ± 0.11	112.13 ± 0.45	11.21
10	2.080	1.936	27.32 ± 0.13	112.16 ± 0.53	9.077
20	2.213	1.377	27.32 ± 0.13	112.40 ± 0.53	6.453
30	2.346	0.818	27.31 ± 0.16	112.82 ± 0.66	3.445
40	2.479	0.259	27.24 ± 0.26	113.32 ± 1.08	0.571
50	2.613	-0.300	27.27 ± 0.24	113.35 ± 1.00	1.218
60	2.746	-0.858	27.32 ± 0.13	112.48 ± 0.54	17.53
70	2.879	-1.417	27.33 ± 0.09	112.14 ± 0.37	18.89
80	3.012	-1.976	27.33 ± 0.08	112.17 ± 0.33	33.93
90	3.145	-2.535	27.33 ± 0.08	111.75 ± 0.33	52.11
100	3.278	-3.094	27.33 ± 0.08	111.33 ± 0.33	72.83

^a deuterium content of the solvent^b SLD calculated with Eq (20)^c contrast, calculated with Eq (21)^d radius of gyration calculated with Eq. (3)^e maximum diameter (D_{max}) obtained from the condition that $p(r) \rightarrow 0$ when $r = D_{max}$ in Eq. (3)^f forward intensity expressed as percents from the total intensity given in Table S9 last column

TABLE S11. Structural parameters of Sb23 subunit.

f_{D_2O} ^a (%)	ρ ^b (10^{10} cm^{-2})	$\Delta\rho$ ^c (10^{10} cm^{-2})	R_g ^d (\AA)	D_{\max} ^e (\AA)	$I(0)$ ^f (cm^{-1})
0	5.681	6.230	13.81 ± 0.02	51.78 ± 0.07	44.21
10	5.817	5.673	13.81 ± 0.02	51.86 ± 0.08	48.83
20	5.952	5.116	13.81 ± 0.02	51.82 ± 0.08	55.66
30	6.088	4.560	13.81 ± 0.03	51.84 ± 0.11	66.34
40	6.223	4.003	13.81 ± 0.02	51.78 ± 0.07	85.45
50	6.358	3.446	13.81 ± 0.02	51.86 ± 0.08	98.83
60	6.494	2.890	13.81 ± 0.02	51.79 ± 0.08	52.67
70	-1.417	2.333	13.81 ± 0.03	52.82 ± 0.11	32.05
80	-1.976	1.776	13.81 ± 0.03	52.85 ± 0.11	17.48
90	-2.535	1.220	13.81 ± 0.05	52.83 ± 0.19	7.73
100	-3.094	0.663	13.80 ± 0.07	52.71 ± 0.27	2.15

^a deuterium content of the solvent^b SLD calculated with Eq (20)^c contrast, calculated with Eq (21)^d radius of gyration calculated with Eq. (3)^e maximum diameter (D_{\max}) obtained from the condition that $p(r) \rightarrow 0$ when $r = D_{\max}$ in Eq. (3) ^f forward intensity expressed as percents from the total intensity given in Table S9 last column